BILINGUAL PUBLISHING CO.
Pioneer of Global Academics Since 1984

Artificial Intelligence Advances
https://ojs.bilpublishing.com/index.php/aia

ARTICLE

Robust PID Controller Design on Quantum Fuzzy Inference: Imperfect KB Quantum Self-Organization Effect-Quantum Supremacy Effect

L.V. Litvintseva[1] V.S. Ulyanov[1] Sergey V. Ulyanov[1,2*]

1. INESYS LLC (EFKO GROUP), Russia
2. Dubna State University, Universitetskaya Str.19, Dubna, Moscow Region, 141980, Russia

ARTICLE INFO

Article history
Received: 11 November 2019
Accepted: 8 April 2020
Published Online: 15 April 2020

Keywords:
PID controller tuning
Quantum fuzzy inference
Intelligent control
Quantum self-organization of imperfect KB
Quantum supremacy

ABSTRACT

The new method of robust self-organized PID controller design based on a quantum fuzzy inference algorithm is proposed. The structure and mechanism of a quantum PID controller (QPID) based on a quantum decision-making logic by using two K-gains of classical PID (with constant K-gains) controllers are investigated. Computational intelligence toolkit as a soft computing technology in learning situations is applied. Benchmark's simulation results of intelligent robust control are demonstrated and analyzed. Quantum supremacy demonstrated.

1. Introduction

A PID controller applied as the instrument in many industrial control applications last 70 years. PID controllers realize a control loop feedback mechanism to control object or plant process variables [1]. They perform an accurate and optimal control in many cases. But PID controllers do not guarantee an optimal and robust control in the case of complex, essentially non-linear and ill-defined structures of controlled objects and in the presence of different stochastic noises.

To improve robustness and control quality capabilities of traditional PID control systems design we have proposed a new approach based on soft and quantum computing toolkit [2].

In our approach a robustness of PID controllers depends on a presence of time dependent PID coefficient's gains, which computed applying Knowledge Bases and a fuzzy inference mechanism. Moreover, in unpredicted situations the robustness of PID controllers depends on a presence of a mechanism of Knowledge Bases self-organization [3]. This mechanism is described as a logical algorithmic process of a value information extraction from hidden layers (possibilities) in classical control laws using quantum decision-making logic [3,4]. The quantum operators, such as superposition, entanglement and interference, give rise to the quantum logic used in quantum computing.

In this article a quantum approach to the design of robust conventional PID controllers is demonstrated. We use a simplified method of a quantum fuzzy inference

**Corresponding Author:*
Sergey V. Ulyanov,
ISESYS LLC (EFKO GROUP), Naberezhnaya Ovchinnikovskaya Str.20 Bld.2, Moscow, Russia;
Email: ulyanovsv@mail.ru

 DOI: https://doi.org/10.30564/aia.v2i1.1401

algorithm, where instead of Knowledge Bases we use disturbed values of K-gains of classical PID controllers. We propose a new mechanism of a quantum PID controller (QPID) design based on a quantum decision-making logic by using two K-gains of classical PID. While in this case membership functions are singletons further instead of naming "quantum fuzzy inference" we will call our method as a "quantum inference" that the particular case of quantum fuzzy inference in [3,4].

Quantum supremacy on Benchmark's simulation results of QPID based robust control for a cart-pole system in unpredicted control situations demonstrated and analyzed.

2. General structure and main ideas of QPID controller design

On Fig. 1, the general structure of control system with quantum PID controller in the presence of external stochastic noise, sensor's time delay and noise in sensor system is shown.

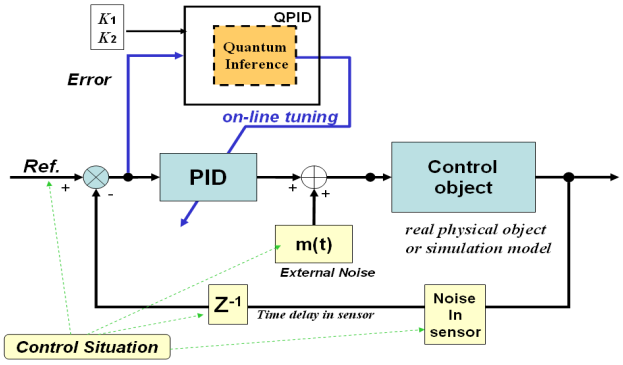

Figure 1. General structure of QPID based on two K-gains of conventional PID and quantum inference.

Consider main ideas of Quantum Inference (QI) [3] based on two PID coefficient gains schedule. We have the following computing steps.

First of all, for two teaching conditions (learning situations) we will design two K-gains, K_1 and K_2, by using genetic algorithm (GA) (so called PID tuning based on GA): $K_1 = \left[k_P^1\ k_D^1\ k_I^1\right]$ and $K_2 = \left[k_P^2\ k_D^2\ k_I^2\right]$.

Remark. See an example of fitness function for GA tuning in the section with simulation results.

By using an artificial stochastic noise disturb obtained K-gains as follows

$$K_{1,2}(t) = \begin{bmatrix} k_P + G_P \cdot \xi(t) \\ k_D + G_D \cdot \xi(t) \\ k_I + G_I \cdot \xi(t)] \end{bmatrix}, \text{where } \xi(t) - \textit{stochastic} \text{ noise with maximal amplitude} = 1 \tag{1}$$

and G_P, G_D, G_I are increasing / decreasing coefficients that can be chosen manually. In two learning situations, simulate a control object motion with new disturbed K-gains and design two probability distributions of K-signals for design of states $|0\rangle$ and $|1\rangle$ in QFI. (See an example of these states preparation in the section with simulation results.)

Realize QFI process based on two K(t)-gains by following steps.

Step 1: Coding. The preparation of all normalized states $|0\rangle$ and $|1\rangle$ for current values of disturbed control signals K_1 and K_2 including:

- a calculation of probability amplitudes α_0, α_1 of states $|0\rangle$ and $|1\rangle$ from histograms;
- a calculation of normalized value of state $|1\rangle$ by using α_1.

Step 2: Choose quantum correlation type for preparation of entangled state. Consider the following quantum correlation (spatial):

$$e_1 e_2 k_P^{1,2} k_D^{1,2} \to k_P^{new} \cdot gain_P;\ \ \dot{e}_1\, \dot{e}_2\, k_D^{1,2} k_I^{1,2} \to k_D^{new} \cdot gain_D;\ \ \ Ie_1\, Ie_2\, k_I^{1,2} k_P^{1,2} \to k_I^{new} \cdot gain_I;$$

where $e, \dot{e}, Ie$ – are control error, derivative and integral of control error correspondingly and $gain_{P(D,I)}$ – are QI scaling factors that can be obtained by GA.

So, a quantum state

$$|a_1 a_2 a_3 a_4 a_5 a_6\rangle = |e_1 e_2 k_P^1(t) k_D^1(t) k_P^2(t)\, k_D^2(t)\rangle \text{ is considered as the entangled state.}$$

Remark. The type of an entangled state is chosen from the list of entangled states types. This list is constructed manually (empirically) and checked by simulation.

Step 3: Superposition and Entanglement. According to the chosen quantum correlation type construct superposition of entangled states. (see an example in the section with simulation results)

Step 4: Interference and measurement. Choose a quantum state

$$|a_1 a_2 a_3 a_4 a_5 a_6\rangle = |e_1(t) e_2(t) k_P^1(t) k_D^1(t) k_P^2(t)\, k_D^2(t)\rangle$$

with the maximum amplitude of probability

$A = \sqrt{P_{e_1}} \cdot \sqrt{P_{e_2}} \cdot \sqrt{P_{k_P^1}} \cdot \sqrt{P_{k_D^1}} \cdot \sqrt{P_{k_P^2}} \cdot \sqrt{P_{k_D^2}}$. Choose subvector $|k_P^1(t) k_D^1(t) k_P^2(t)\, k_D^2(t)\rangle$.

Step 5: Decoding.

Calculate normalized output as a norm of subvector of the chosen quantum state as follows:

$$k_P^{new}(t) = \frac{1}{\sqrt{2^{n-2}}} \sqrt{\langle a_3 \ldots a_n | a_3 \ldots a_n \rangle} = \frac{1}{\sqrt{2^{n-2}}} \sqrt{\sum_{i=3}^{n} (a_i)^2}, \quad n = 6 \tag{2}$$

DOI: https://doi.org/10.30564/aia.v2i1.1401

Step 6: Denormalization.

Calculate final (denormalized) output result as follows:

$$k_P^{output} = k_P^{new}(t) \cdot gain_P, \quad k_D^{output} = k_D^{new}(t) \cdot gain_D, \quad k_I^{output} = k_I^{new}(t) \cdot gain_I. \tag{3}$$

Step 7: Find robust QI scaling gains $\{gain_P, gain_D, gain_I\}$ based on GA and a chosen fitness function. (See a fitness function example in the section with simulation results).

Let us consider the Benchmark of control object and investigate robustness and self-organization properties of proposed QPID controller based on developed QI algorithm.

3. Quantum PID based smart control design: example of Benchmark simulation results

Consider a QPID controller design for a typical benchmark of globally unstable dynamic system (a so called «cart-pole» system). The geometrical model of the «cart-pole» dynamic system is shown on Fig. 2.

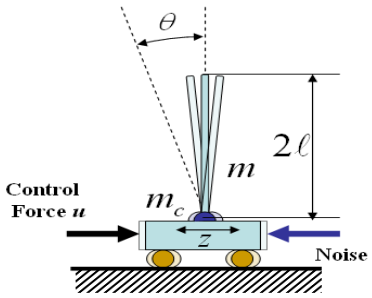

Figure 2. Geometrical model of cart-pole system

Control problem: acting by a control force on the cart, keep the Pole motion vertical and stable (pendulum angle $\theta = 0$) in spite of different environment conditions.

Our control goal is to balance the pole with limited cart's position and velocity, with limited control force and in the presence of stochastic noises and sensor's delay time.

These conditions and constraints in the search of optimal solutions are intractable task for conventional control system theory.

The inverted pendulum (called also a pole) problem control is described by second-order differential equations system for computing control force that to be used for moving the cart:

$$\ddot{\theta} = \frac{g\sin\theta + \cos\theta\left(\frac{+(u+\xi(t)) + \{+a_1\dot{z} + a_2 z\} - ml\dot{\theta}^2\sin\theta}{m_c + m}\right) - k\dot{\theta}}{l\left(\frac{4}{3} - \frac{m\cos^2\theta}{m_c + m}\right)} \tag{4}$$

$$\ddot{z} = \frac{u + \xi(t) + \{-a_1\dot{z} - a_2 z\} + ml(\dot{\theta}^2\sin\theta - \ddot{\theta}\cos\theta)}{m_c + m}, \tag{5}$$

where z and θ are generalized coordinate; g is the acceleration due to gravity (usually $9.8\ m/\sec^2$), m_c is the mass of the cart, m is the mass of inverted pendulum (called also as a pole), l is the half-length of the pendulum, k and a_1 are friction coefficients in z and θ correspondingly, a_2 is a spring force that bounded the cart motion, $\xi(t)$ is external stochastic noise and u is the applied control force in Newton's.

According to the control system structure (shown in Fig.1) we have at the low level one PID controller which controls a cart motion so that the Pole doesn't fail down.

For the pole stabilization ($\theta = 0$) we introduce a reference signal for z as following:

z_{ref} is a projection on axis z of the center of gravity of the pole. It must be equal 0 for stabilization the pole motion.

We can represent z_{ref} as $z_{ref} = -w \cdot l \cdot \sin\theta$, where w is some scaling parameter. If $\theta \to 0; z_{ref} \to 0$.

We also introduce constraints on the center of gravity projection: $|z_{ref}| \le 1$ and on applied control force: $\lfloor u \rfloor \le 5\,(N)$. We also consider a presence of a time delay in a measurement system.

Thus, one PID controller through cart motion (first DOF) controls a position of the inverted pendulum (second DOF), i.e. one PID controller control 2DOF control object through energy transfer phenomena from one DOF to another applying non-linear interrelations in Eqs (1) and (2).

3.1 Teaching conditions for PID tuning

In Table 1 model parameters for the chosen control object are described.

Table 1. Cart-Pole System: Model Parameters

m_C [kg]	m [kg]	l [m]	Damping in ɵ, k	Damping in z, a_2	Spring force coefficient in dz, a_1
1.0	0.1	0.5	0.4	0.1	5.0

We also take the following Cart-Pole initial conditions: the pole angle $\theta = {}^{[10\ ;\ 0.1]}$ in degrees; cart position z = $^{[0;\ 0]}$ in m.

Constraints: a cart position: -1.0 < z < 1.0 [m]; control force: -5.0 < u < 5.0 [N].

Sensor's delay time = 0.001 sec.

We will use two stochastic external noises (shown on Fig. 3) for two teaching conditions with different prob-

 DOI: https://doi.org/10.30564/aia.v2i1.1401

ability distribution density functions: Gaussian noise (symmetric probability distribution density function) and Rayleign noise (with nonsymmetrical probability distribution density function).

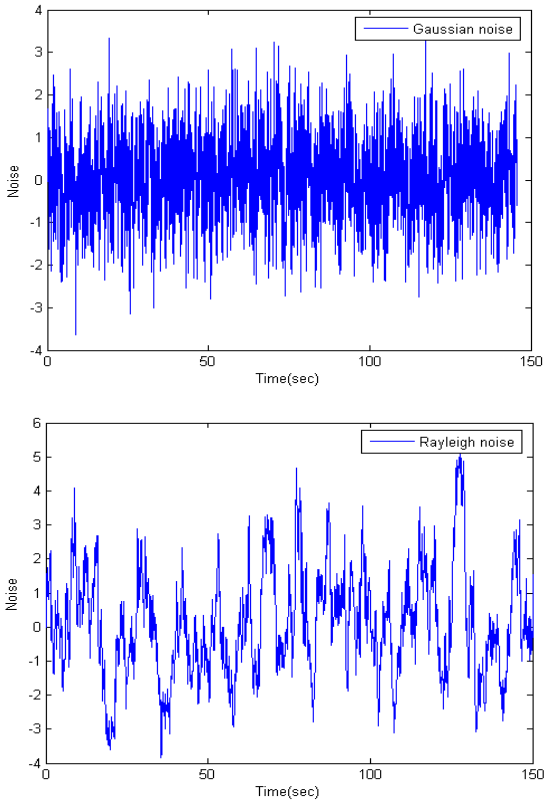

Figure 3. External stochastic noises in teaching control situations.

According to the step's description of QI algorithm above at first stage let us find for two teaching conditions two K-gains K_1 and K_2 by using GA. We have worked with a mathematical model of the cart-pole system represented in Matlab / Simulink.

3.2 PID tuning based on GA. Design time dependent K-gains for QPID

Teaching conditions 1 with Gaussian noise (named as TS1).

In order to apply GA, we must define a fitness function and a search space for GA. Search space for PID gains K = [100 100 100] is defined from preliminary simulations with PID control. We define the following Fitness Function (y) for GA tuning: $y = -\sum_t \theta^2 - \sum_t \dot{\theta}^2$. In Matlab toolkit, this fitness function is represented as following:

$$y = -sum(\text{simoutX}(:,1).\hat{}\,2)/\text{Norm} - sum(\text{simoutX}(:,2).\hat{}\,2)/\text{Norm}$$

where simoutX(:,1) is a vector of angle (ϴ) values; simoutX(:,2) is a vector of angular velocity values and Norm is a length of these vectors.

As result of GA tuning, we obtained the following value K_1 = [82.7 13.6 9.4]. We will call PID with K_1 as PID_1.

Now according to (1) we disturb K_1 gains as shown in Matlab model represented on Fig. 4 (a). (see right block).

QI process in QPID block in Matlab model on Fig. 4 (b) demonstrated.

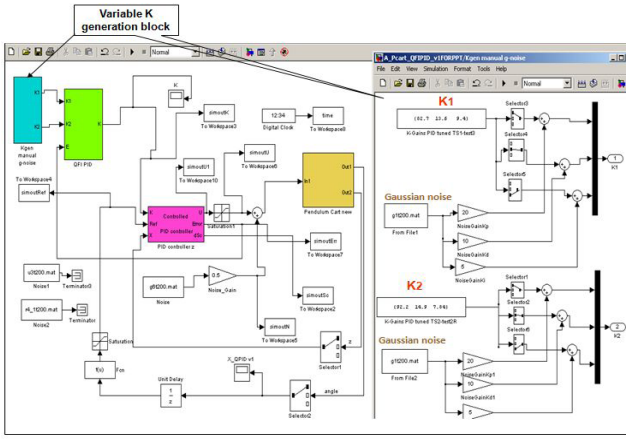

Figure 4 (a). The Matlab structure of QPID based control system.

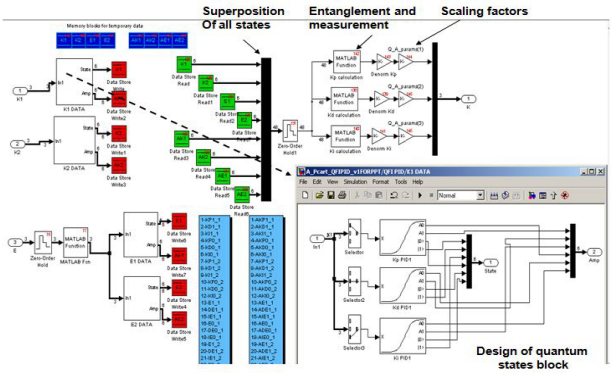

Figure 4 (b). QI process in QPID block in Matlab model.

By the Matlab simulation we define manually (it is easy to do) increasing noise coefficients G_P, G_D, G_I so that $K_1(t)$ and $K_2(t)$ give robust control (the Pole doesn't fall down).

If the Pole fails down, we take smaller G_P, G_D, G_I and check again robustness. Finally, we choose bigger G_P, G_D, G_I that give $K_1(t)$ and $K_2(t)$ with robust control (The Pole doesn't fall down).

Finally, we have the following time dependent $K_1(t)$ for our QPID.

1. TS1 control situation

DOI: https://doi.org/10.30564/aia.v2i1.1401

$$K_1(t)=\begin{bmatrix} k_p+gain_p\cdot\xi(t) \\ k_d+gain_d\cdot\xi(t) \\ k_i+gain_i\cdot\xi(t)] \end{bmatrix}=\begin{bmatrix} 82.7+20\cdot\xi(t) \\ 13.6+10\cdot\xi(t) \\ 9.4+5\cdot\xi(t)] \end{bmatrix},$$

where $\xi(t)$ – Gaussian noise with maximal amplitude = 1.

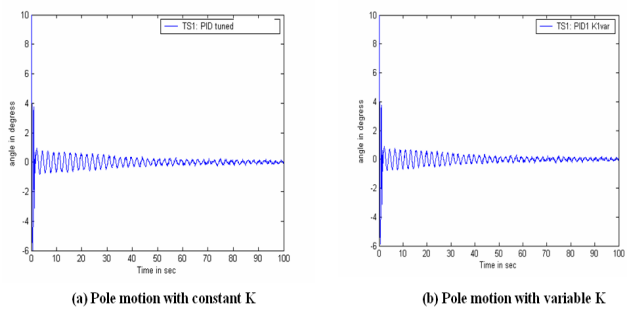

(a) Pole motion with constant K (b) Pole motion with variable K

Figure 5. Teaching conditions 1: Pole motion with constant and disturbed K-gains of PID_1

Now let us see on the motion of our control object under constant and variable (time dependent) K_1-gains as shown on Fig. 5. We see that the pole motion is stable in both cases.

On Fig. 6 the disturbed K-gains of PID_1 (called as control laws) are shown.

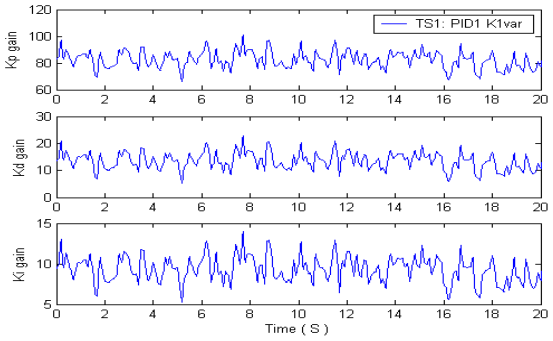

Figure 6. Teaching conditions 1: Control laws.

Teaching conditions 2 with Rayleigh noise (named as TS2). As result of GA tuning, we obtained K_2 = [92.2 14.9 7.84]. We will call PID with K_2 as PID_2. Analogically we obtain the following time depending $K_2(t)$.

$$K_2(t)=\begin{bmatrix} k_p+gain_p\cdot\xi(t) \\ k_d+gain_d\cdot\xi(t) \\ k_i+gain_i\cdot\xi(t)] \end{bmatrix}=\begin{bmatrix} 92.2+20\cdot\xi(t) \\ 14.9+10\cdot\xi(t) \\ 7.84+5\cdot\xi(t)] \end{bmatrix},$$

where $\xi(t)$ – gaussian noise with maximal amplitude = 1.

Simulation results on Fig. 6 show the pole motion.

Remark. On Fig. 7 and all others below, we will denote pole angle θ as x.

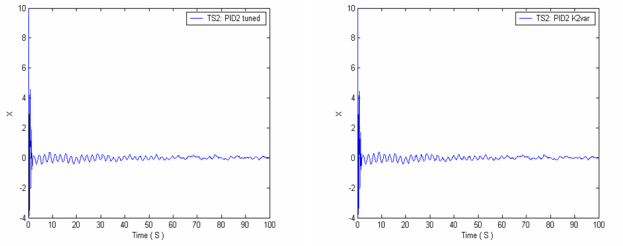

(a) Pole motion with constant K (b) Pole motion with variable K

Figure 7. Teaching conditions 2: Pole motion with constant and disturbed K-gains of PID_2

In this case also simulation results show that the pole motion is stable in both cases.

On Fig. 8 the disturbed K-gains of PID_2 (called as control laws) are shown.

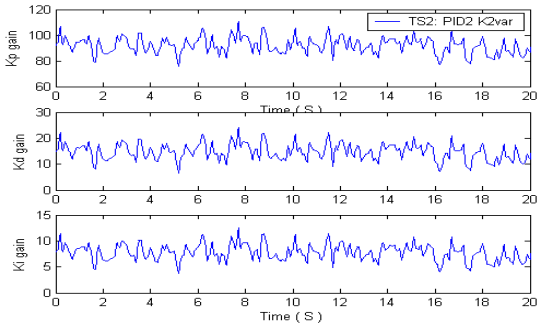

Figure 8. Teaching conditions 2: Control laws.

Conclusion: The simulation results (Figs. 5-8) show that the pole motion is stable in both cases (with constant K_1 and K_2 and with time-depending K_1 and K_2) . It means that we can use disturbed K-values for further calculations in QPID.

QPID controller based on a new type of computing

We developed special tools for Quantum Fuzzy and Quantum PID inference based on QC optimizer ($QCOptKB^{TM}$) [4,6].

$QCOptKB^{TM}$ toolkit allows to control as a physical system and a mathematical model of a control object as shown on Fig. 9.

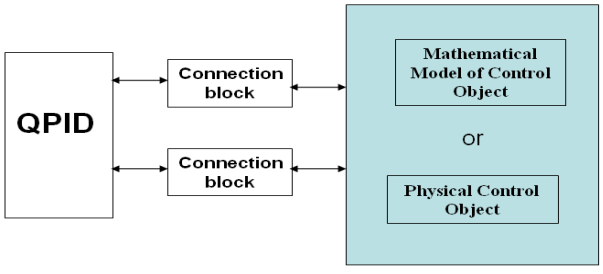

Figure 9. QPID controller connected with a control object.

We will work with mathematical model of control ob-

ject represented in Matlab / Simulink. Control loop with QPID is shown on Fig. 10.

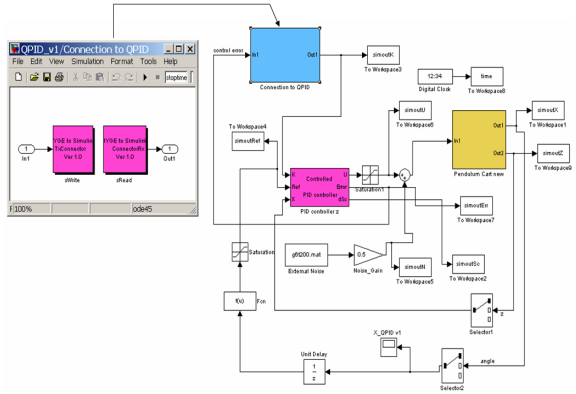

Figure 10. Matlab / Simulink model of control object with control loop based on QPID.

Calculations corresponding to QI based on two K-gains are realized in the block QPID by applying QC Optimizer toolkit.

3.3 QPID in terms of QC optimizer tool

On Figs 11a and 11b, internal structure of QPID in terms of our toolkit is shown.

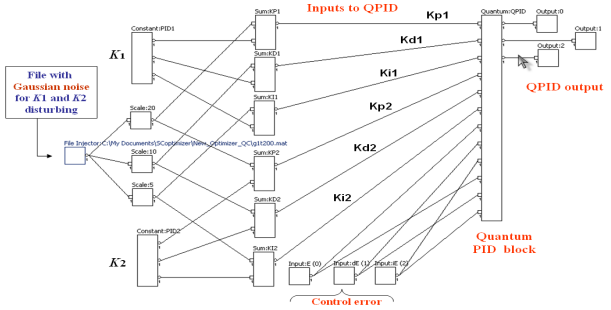

Figure 11a. QPID structure in terms of QC Optimizer tools

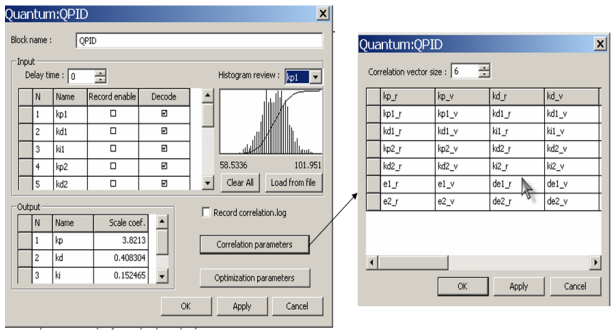

Figure 11b. QPID structure. Internal layer in terms of QC Optimizer tool.

On Fig. 11b internal structure of QPID block is shown. In this block the following items are described:

- names of input variables $k_{P(D,I)}^{1,2}$, where indexes 1, 2 denotes PID_1 and PID_2 (or K_1 and K_2);
- names of output variables $k_{P(D,I)}$;
- histograms for each input variable representing probability distribution of the given input;
- QI scaling coefficients for calculation output values (that is founded by GA for teaching conditions and then used for all control situations);
- knob «correlation parameters» is used for the choice of quantum correlation type description.

For example, let us use the following quantum correlations (spatial):

$$e_1 e_2 k_P^{1,2} k_D^{1,2} \to k_P^{new}; \quad e_1\, \dot{e}_2\, k_D^{1,2} k_I^{1,2} \to k_D^{new}; \quad Ie_1\, Ie_2\, k_I^{1,2} k_P^{1,2} \to k_I^{new}.$$

By using GA and chosen quantum correlation we obtained the following QI scaling coefficients: Q_A_params = 2.4200 0.3320 0.1000.

Remark. A fitness function is the same as in PID tuning. Only search space is different. In the case of GA for QI scaling gains search space is as the formula bar displays the contents.

Now investigate robustness properties of designed QPID based on QI with the given correlations in different control situations.

3.4 Investigation of self-organization capability of Quantum PID Control based on two PID controllers

We will consider the following controllers:

o PID_1 controller with constant gains K_1 = [82.7 13.6 9.4];

o PID_2 controller with constant gains K_2 = [92.2 14.9 7.84];

o QPID controller based on QI with K_1 and K_2.

Consider now behavior of control object in teaching and modeled unpredicted control situations and investigate robustness property of designed controllers.

Investigation of different types of quantum correlations: Spatial correlations.

TS1: Comparison of QPID, PID_1 and PID_2 control performances.

Figures 12-14 demonstrate simulation results in the first teaching control situation.

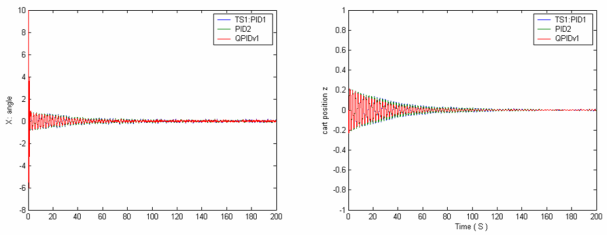

Figure 12. The Pole motion (left) and cart motion (right) comparison.

DOI: https://doi.org/10.30564/aia.v2i1.1401

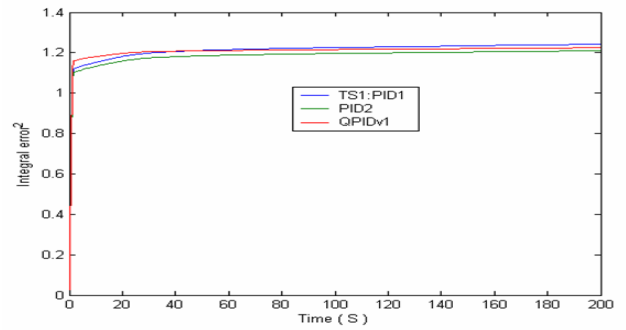

Figure 13. The integral control errors.

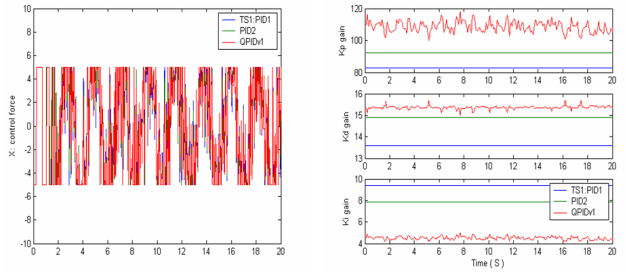

Figure 14. The control force and control laws

Conclusion: all considered controllers are successful to balance the Pole in TS1 situation.

TS2: Comparison of QPID, PID_1 and PID_2 control performance.

On Figs 15 – 17, a behavior of the Cart-Pole system in the teaching conditions TS2 is shown.

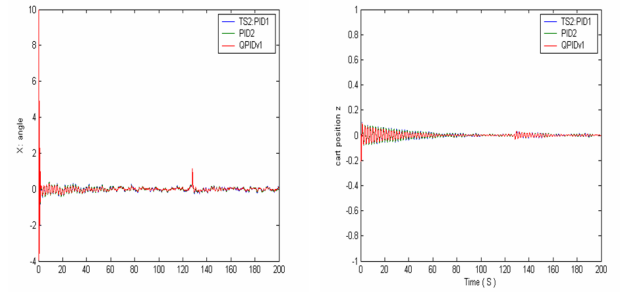

Figure 15. The Pole motion (left) and cart motion (right) comparison in TS2 situation

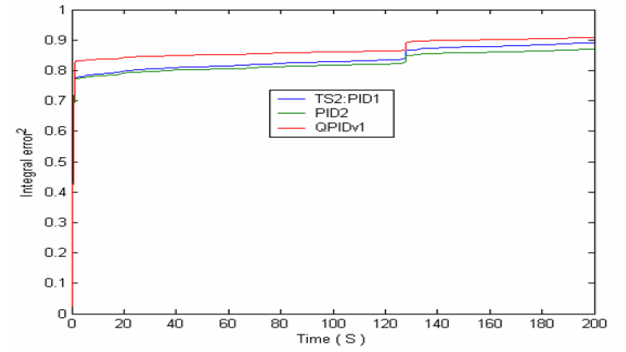

Figure 16. The Integral control errors.

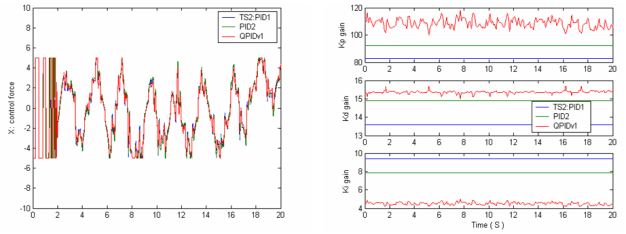

Figure 17. The control force and control laws in TS2 situation

Conclusion: all considered controllers are successful to balance the Pole in TS2 situation.

3.5 Investigation of self-organization capability of chosen QFI

In the Table 2 modeled unpredicted control situations (Class 1) are shown.

Table 2. Class 1 of modeled unpredicted control situations

New 1 control situation (in legend **S**1)	**New 2 control situation** (in legend **S**1a)	**New 3 control situation** (in legend **S**1b)
External noise: *Rayleigh* (TS2 teaching noise); New sensor's time delay = 0.005 sec; Internal sensor noise: Gaussian noise with amplitude = 0.015; TS model parameters	External noise: *Rayleigh* (TS2 teaching noise); New sensor's time delay = 0.005 sec; Internal sensor noise: Gaussian noise with amplitude = 0.015; *New model parameter a*2 = 8	External noise: *Rayleigh* (TS2 teaching noise); Sensor's time delay = 0.001 sec; Internal sensor noise: Gaussian noise with amplitude = 0.01; *New model parameter a*2 = 6

Let us investigate a robustness of the proposed QPID model in a new control environment (Table 2).

New 1 control situation. Figures 18 – 20 show the simulation results in unpredicted control situation Remark. In a plot presentation below "New1" is denoted as S1. See the Table 2.

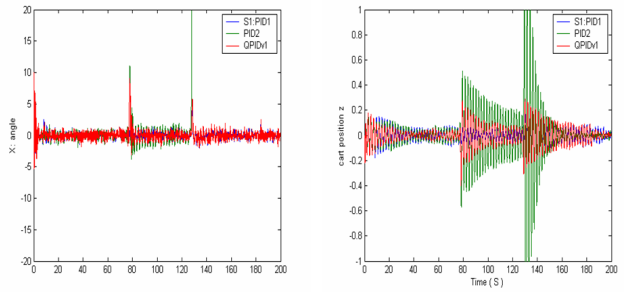

Figure 18. The Pole motion (left) and the cart motion (right) comparison in New 1 situation.

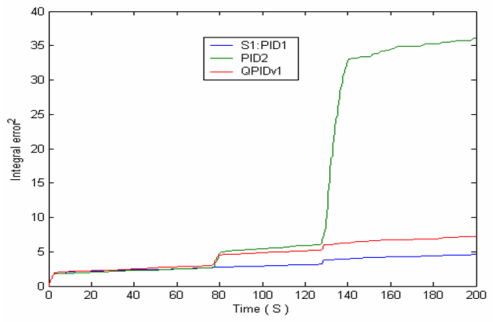

Figure 19. The Integral control error in New 1 situation.

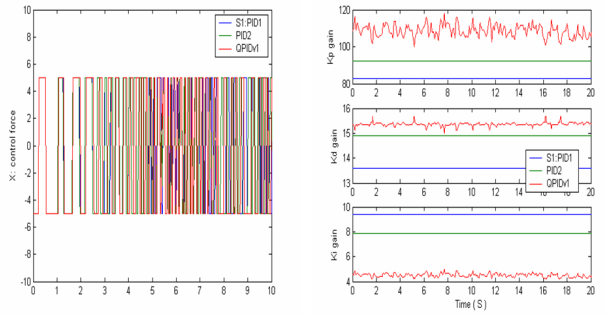

Figure 20. The control force and control laws in New 1 situation.

The presentation of control laws and control forces in a point where the Pole falls down.

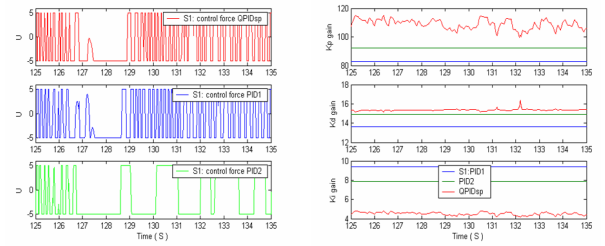

Figure 21. The control force and control laws in New 1 situation

Conclusion: QPID and PID_1 controllers are successful to balance the Pole in New 1 situation. PID_2 controller is unsuccessful to balance the Pole in New 1 situation.

New 2 control situation. Figures 22 – 25 show the simulation results of the cart-pole motion in New2 unpredicted situation.

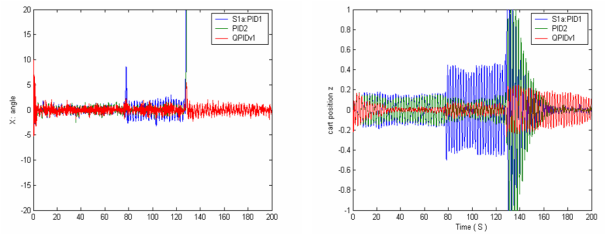

Figure 22. The Pole motion (left) and cart motion (right) comparison in New 2 situation.

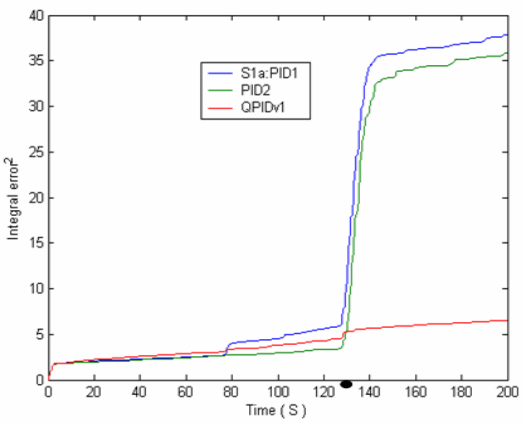

Figure 23. Integral control error in New 2 situation.

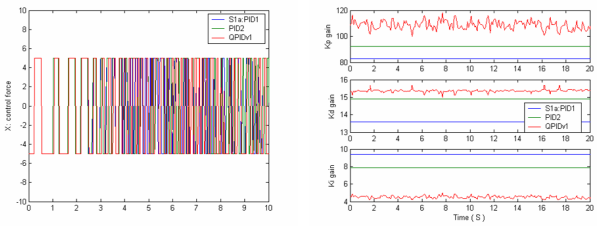

Figure 24. The control force and control laws in New 2 situation

The representation of control laws and control forces in a point where the Pole falls down.

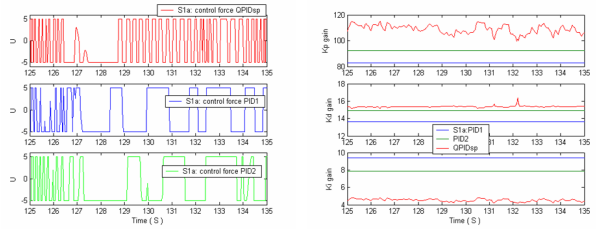

Figure 25. The control force and control laws in New 2 situation

Conclusion: QPID controller is successful to balance the Pole in New 2 situation. PID_1 and PID_2 controllers are unsuccessful to balance the Pole in New 2 situation.

New 3 control situation. Figures 26 – 28 show the simulation results of the cart-pole motion in New3 unpredicted situation.

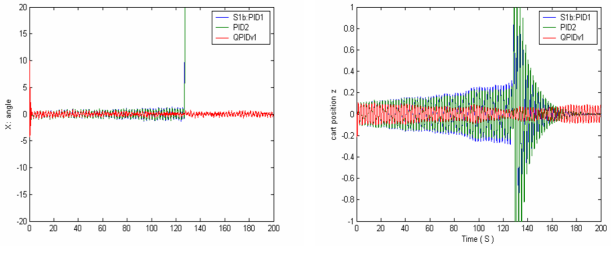

Figure 26. The Pole motion (left) and cart motion (right) comparison in New 3 situation.

DOI: https://doi.org/10.30564/aia.v2i1.1401

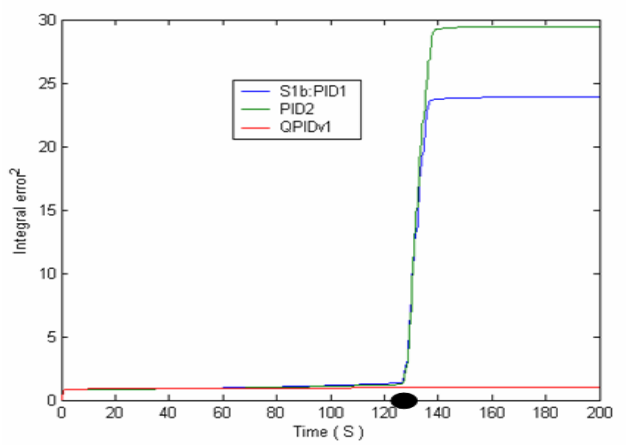

Figure 27. The integral control error in New 3 situation

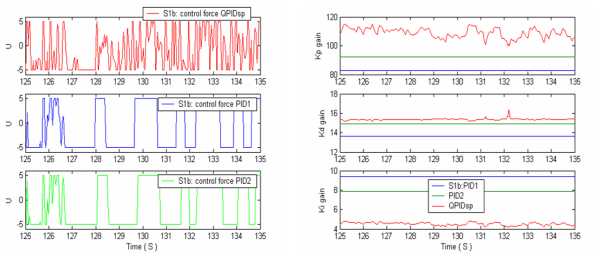

Figure 28. Control forces and control laws in New 3 situation

Conclusion: QPID controller is successful to balance the Pole in New 3 situation. PID_1 and PID_2 controllers are unsuccessful to balance the Pole in New 3 situation.

Final conclusions:

- QPID controller is robust in all situations of class1;
- PID_1 controller is robust in New 1 situation only;
- PID_2 controller is not robust in class 1 situations;
- QPID based on new type of calculations increases robustness of designed PID controllers.

3.6 Investigation of different types of quantum correlations: Temporal correlations

Investigate now a robustness of temporal quantum correlations and compare with the spatial type of QI for the given control object. Let us consider QI with the following temporal quantum correlations as follows:

$$e_1 e_2 k_P^{1,2}(t) k_P^{1,2}(t-\Delta t) \to k_P^{new}(t) \cdot gain_P; \quad \dot{e}_1 \dot{e}_2 k_D^{1,2}(t) k_D^{1,2}(t-\Delta t) \to k_D^{new}(t) \cdot gain_D;$$
$$Ie_1 Ie_2 k_I^{1,2}(t) k_I^{1,2}(t-\Delta t) \to k_I^{new}(t) \cdot gain_I.$$

On Fig. 29, a cart-pole dynamic motion in TS1 situation is shown for different values of time correlation parameter $\Delta t = 0.25$ sec and 0.05 sec.

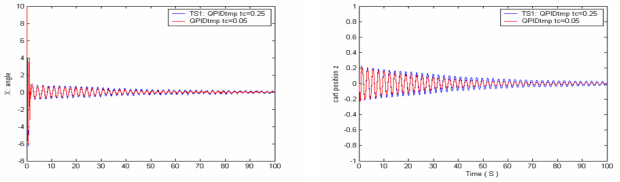

Figure 29. The Pole motion (left) and cart motion (right) comparison in TS1 situation – Temporal quantum correlations.

Check now a robustness of temporal correlations.

On Figs. 30 -31 the cart-pole dynamic motion in New 1 control situation (in legend S1) is shown for different values of time correlation parameter $\Delta t = 0.25$ sec and 0.05 sec. You can see that the Pole falls down.

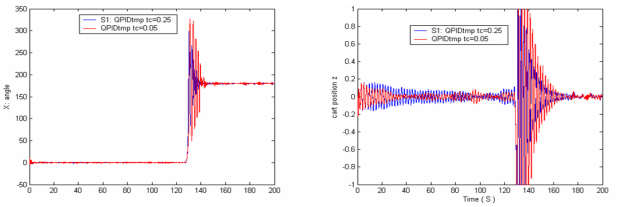

Figure 27. Pole motion (left) and cart motion (right) comparison in New 1 situation: Temporal quantum correlations. Pole falls down

3.7 Comparison QPID control performance under spatial and temporal correlations

Consider dynamic motion and control laws comparison (around the point, where the Pole falls down).

Figures 30 and 31 show results of the comparison.

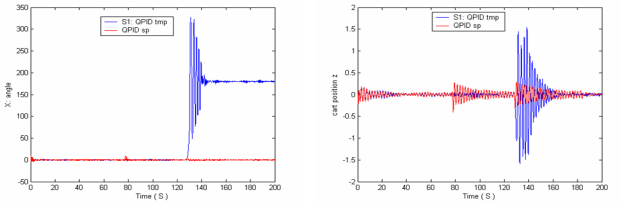

Figure 30. Pole motion (left) and cart motion (right) comparison.

Conclusion: QPID with temporal correlations is not robust in New 1 situation. So, choose the QI based on spatial quantum correlation as a best candidate the for robust QPID realization.

Consider now a new class of modeled unpredicted control situations (Class 2) shown in Table 3. For the new control situations (New 6 and New 7) the external uniform noise is used (Fig. 31).

 DOI: https://doi.org/10.30564/aia.v2i1.1401

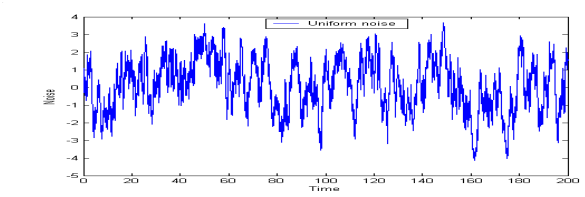

Figure 31. External Uniform noise applied in New 6 and New 7 control situations.

Table 3. Class 2 of modeled unpredicted control situations

New 4 control situation (in legend **S2**) External noise: *Gaussian* (TS1 teaching noise); New sensor's time delay = 0.004 sec; Internal sensor noise: Gaussian noise with amplitude = 0.015; TS model parameters	**New 5 control situation** (in legend **S2a**) External noise: *Gaussian* (TS1 teaching noise); New sensor's time delay = 0.004 sec; Internal sensor noise: Gaussian noise with amplitude = 0.015; *New model parameter a*2 = 8
New 6 control situation (in legend **S3**) New external noise: *Uniform* (Fig.13.32); New sensor's time delay = 0.005 sec; Internal sensor noise: Gaussian noise with amplitude = 0.015; TS model parameters	**New 7 control situation** (in legend **S3b**) New external noise: *Uniform* (Fig.13.32); New sensor's time delay = 0.005 sec; Internal sensor noise: Gaussian noise with amplitude = 0.015; *New model parameter a*2 = 8

New 4 control situation.

Figures 32 – 34 show the simulation results of the cart-pole motion in the New4 unpredicted situation.

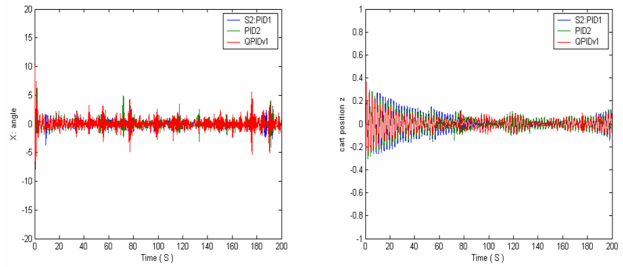

Figure 32. Pole motion (left) and cart motion (right) comparison in New 4 situation.

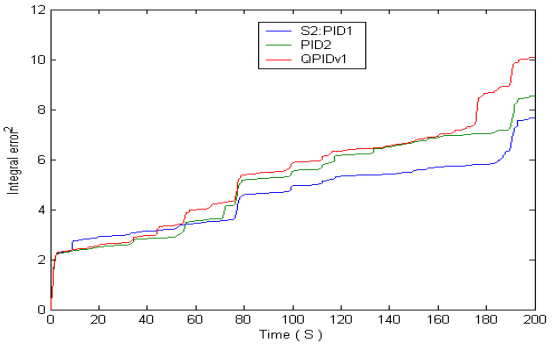

Figure 33. The Integral control error in New 4 situation.

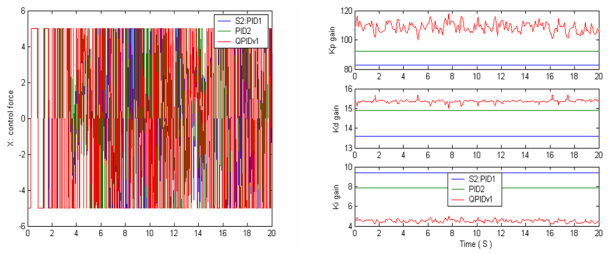

Figure 34. Control force and control laws in New 4 situation.

Conclusion: all controllers are successful to balance the Pole in New 4 situation.

New 5 control situation.

Figures 35 – 37 show the simulation results of the cart-pole motion in the New5 unpredicted situation.

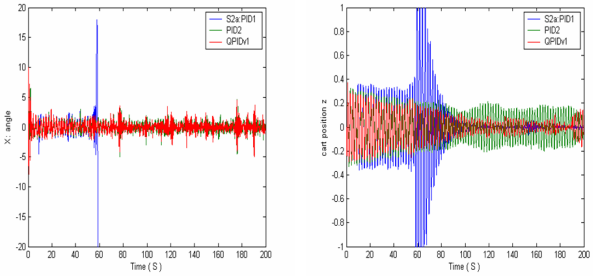

Figure 35. The Pole motion (left) and cart motion (right) comparison in New 5 situation.

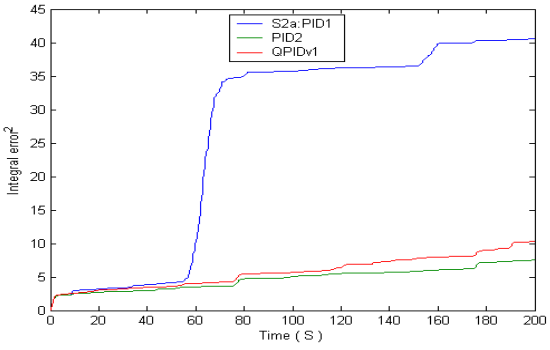

Figure 36. Integral control error in New 5 situation.

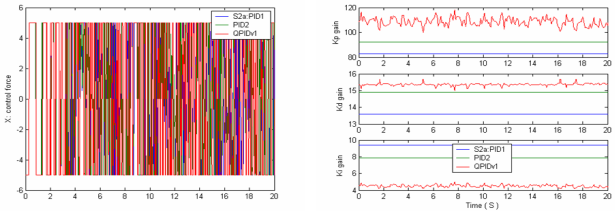

Figure 37. Control force and control laws in New 5 situation.

Conclusion: QPID controller and PID_2 controllers are successful to balance the Pole in New 5 situation. PID_1 controller is unsuccessful to balance the Pole in New 5 situation.

DOI: https://doi.org/10.30564/aia.v2i1.1401

New 6 control situation.

Figures 38 – 40 show the simulation results of the cart-pole motion in the New6 unpredicted situation where a new type of external noise is - Uniform (Fig.31);

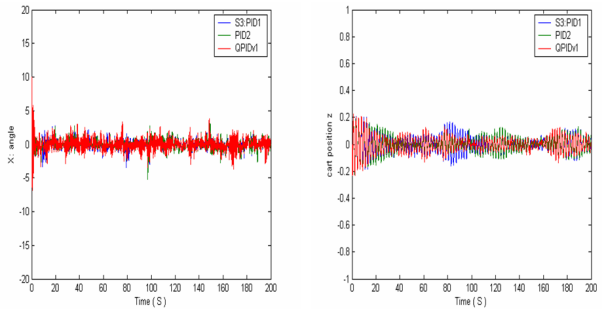

Figure 40. The Pole motion (left) and cart motion (right) comparison in New 6 situation.

Conclusion: All considered controllers are successful to balance the Pole in New 6 situation.

New 7 control situation

The cart-pole motion in the New6 unpredicted situation is shown on Fig.41.

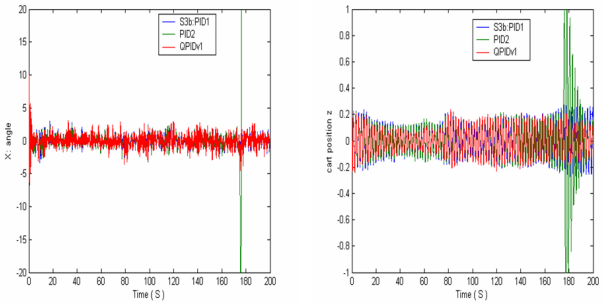

Figure 41. Pole motion (left) and cart motion (right) comparison in New 7 situation.

Conclusion: QPID and PID_1 controllers are successful to balance the Pole in New 7 situation. PID2 controller is unsuccessful to balance the Pole in New 7 situation.

Some important remarks

As shown on Fig. 42 and Fig. 43 below, control laws of QPID in teaching conditions and in new control situations are similar.

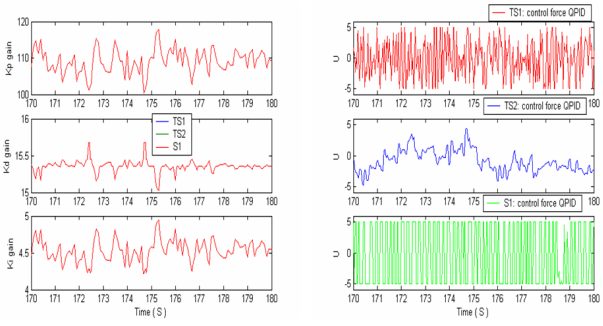

Figure 42. Control laws and control forces in teaching conditions (TS1 and TS2) and in New 1 situation

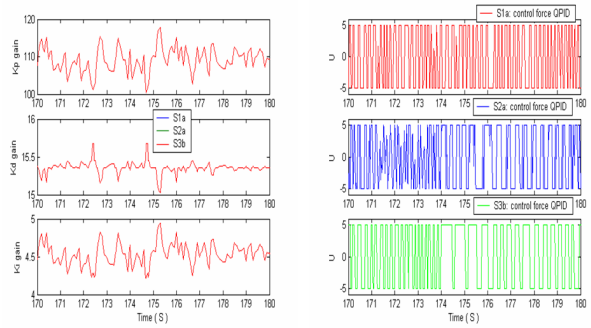

Figure 43. Control laws and control forces in New 2, New 5, New 7 situations

Thus, we have used constant values K_1 and K_2 of classical PID in order to obtain variable K-gains of QPID. Constant K_1 and K_2 of classical PID are not changed when control situation is changed, variable QPID K-gains also is not changed when control situation is changed. If so, let us take average values from obtained QPID K-gains. By this way we can receive new PID that we will call as PID-average.

If we take $K = \max_t K_{QPID}$, then we obtain new controller named as PID-max.

Let us testing robustness of new obtained controllers in chosen control situation (New 2 or in legend S1a). On Fig. 44 comparison of cart-pole motion under three types of control:

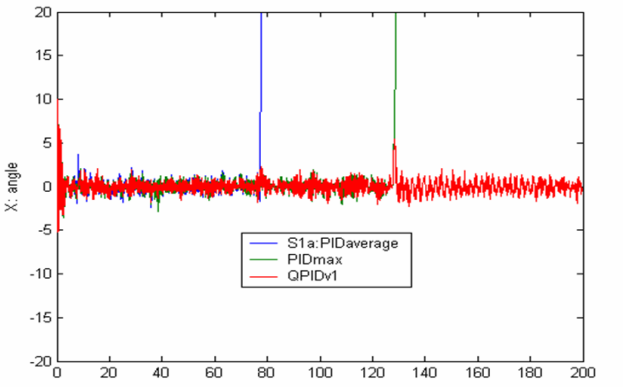

Figure 44. Pole motion under three types of control

- QPID with variable (time dependent) K-gains obtained by on-line QFI process;

- PID-average with constant gains K= [108.8507 15.3634 4.5209];

- PID-max with constant gains K= [119.2325 16.3510 5.1046].

Simulation results show that PID-average and PID-max controllers with constant gains are incapable to balance a Pole in the chosen control situation.

We have seen that constant K-gains obtained from

 DOI: https://doi.org/10.30564/aia.v2i1.1401

quantum inference cannot control pendulum motion in the new situation. But variable K-gains can do it. Thus, we have principally new computing process.

4. Conclusions

Main ideas, algorithm and simulation results of QPID controller are described.

o By applying the typical benchmark of a globally unstable control object (as a "cart-pole" system) a comparison of two types of PID control have been considered: 1) PID with constant coefficients gains; and 2) QPID with time dependent coefficients gains computed on the base of a proposed quantum inference algorithm.

o Simulation results allow us to make the following conclusion: control systems with constant coefficients gains are attractive for many conventional control situations. However due to the constancy of control parameters, standard PID controllers do not guarantee a robust control in unpredicted control situations.

o For practical applications, when we have deal only with PID controllers, we may increase a robustness of control system by using the quantum inference model.

o For achievement the robustness of QPID controller only two sets of PID constant K-gains are needed.

o Simulation results show good robustness properties of QPID based on quantum inference block.

Further investigations of different QPID models are considered as useful and important [7].

References

[1] R. E. Bellman, Adaptive Control Processes: A Guided Tour. Princeton University Press. 2015. ISBN 9781400874668.

[2] L. V. Litvintseva, S. V. Ulyanov, V. S. Ulyanov, Design of robust knowledge bases of fuzzy controllers for intelligent control of substantially nonlinear dynamic systems: II. A soft computing optimizer and robustness of intelligent control systems. J. of Computer and Systems Sci. Intern. 2006. (45) 5. 744-771 DOI: 10.1134/S106423070605008X.

[3] L. V. Litvintseva, S. V. Ulyanov, Intelligent control systems. I. Quantum computing and self-organization algorithm. J. of Computer and Systems Sci. Intern. 2009. (48) 6. 946-984 DOI: 10.1134/S1064230709060112.

[4] L. V. Litvintseva, S. V. Ulyanov, Intelligent control systems. II. Design of self-organized robust knowledge bases in contingency control situations. J. of Computer and Systems Sci. Intern. 2011. (50) 2. 250-292 DOI: 10.1134/S1064230710061036.

[5] S.V. Ulyanov, M. Feng, K. Yamafuji, T. Fukuda, Stochastic analysis of time-invariant non-linear dynamic systems. Pt 1: the Fokker-Planck-Kolmogorov equation approach in stochastic mechanic. Prob. Eng. Mech., 1998, Vol. 13, № 3, Pts 1&2. p. 183 – 203; 205-226.

[6] S.V. Ulyanov, Self-organization quantum robust control methods and systems for situations with uncertainty and risk. US Patent No 8, 0345 874. – 2014.

[7] S.V. Ulyanov, Quantum fast algorithm computational intelligence Pt I: SW / HW smart toolkit. Artificial Intelligence Advances. 2019. Vol. 1. No 1. Pp. 18-43 (URL: https://doi.org/10.30564/aia.v1i1.619).

DOI: https://doi.org/10.30564/aia.v2i1.1401